Simulation of power system transients using state-space grouping through nodal analysis

Jean Mahseredjian, Christian Dufour, Ulas Karaagac and Jean Bélanger

***Abstract*— The paper demonstrates that state-space grouping can be used to allow a modulation of computational burden between state-space and nodal equations. In addition to off-line examples, the described methodology offers many advantages for real-time simulation methods. In fact it provides a solution to otherwise unrealizable simulations in real-time mode.**

***Index Terms*—state-space, nodal analysis, electromagnetic transients, real-time.**

I. INTRODUCTION

The computation of electromagnetic transients is based on numerical methods for the formulation and solution of network equations. The most widely used methods fall into two categories: the state-space and nodal analysis formulations. State-space equations are used in [1] for inserting electrical circuit equations into the Simulink solver. Nodal equations are widely used in EMT-type (Electromagnetic Transients) applications, such as [2]. Some real-time simulator technologies are also based on the nodal formulation [3][4]. The modified-augmented-nodal analysis (MANA) has been introduced in [5],[6] for eliminating topological restrictions from the classical nodal analysis approach. Since MANA equations are more general they are referred to hereinafter in this paper.

MANA equations are assembled efficiently and directly after discretizing all circuit devices with a numerical integration rule such as trapezoidal integration. Such equations are suitable for simulating very large networks through sparse matrix methods.

In state-space equations the numerical integration technique is selected after formulation, which simplifies the programming of variable time-step integration techniques. In addition state-space representation can be particularly powerful for controller design methods [1]. The automatic synthesis process of state-space matrices requires the determination of the network topological proper-tree and can become extremely inefficient for large networks. Complications can arise for the simultaneous solution of nonlinear models, for the simulation of large networks and for large numbers of states in some model equations.

Some variations of the nodal approach are based on the concept of group separation for increasing efficiency and flexibility. In [7] the use of groups provides a technique for diminishing the number of nodal points and consequently the size of the system matrix for real-time computations [8]. In [9] the compensation method allows separating circuits and solving them independently. The compensation method is non-iterative when the solved circuits are linear. A similar idea for the linear case is used in [10] for reducing the number of nodal connection points. In [11] state-space equations are also used for this purpose.

The inclusion of state-space equations into nodal equations has been applied in [12] (see also [13]) for the purpose of model circuit synthesis from fitted measurements.

This paper presents the theoretical formulations and backgrounds through which MANA and state-space equations can be simultaneously combined for arbitrary network topologies. The proposed combination allows eliminating several modeling limitations in state-space based solvers. It also allows creating state-space groups that can be maintained independently thus avoiding problematic (memory limited) massive pre-calculations of state-space matrix sets for all possible switch position combinations [14]. In addition, each state-space group uses its own automatic formulation of state-space matrices which obviously reduces the formulation time when compared to unique state-space equations of the complete system without grouping.

The method proposed in this paper contributes to the improvement of state-space based power system simulation solvers. It notably offers important advantages for real-time applications. The paper follows the initial works presented in [15] and contributes a new theoretical analysis, generalization and new simulation results.

The reference state-space and MANA solvers used in this paper are those presented in [1] and [16] respectively.

II. THEORETICAL FORMULATION

A. Hybrid analysis

Hybrid analysis [17], [18] is a generic method for formulating network equations. It can be used to derive other formulations and to create relations between different circuit

Christian Dufour is with Opal-RT Technologies, 1751 Richardson, Montréal (Québec), Canada, H3K 1G6
Jean Mahseredjian and Ulas Karaagac are with École Polytechnique de Montréal, Campus Université de Montréal, 2900, Édouard-Montpetit, Montréal (Québec), Canada, H3T 1J4 (corresponding author, 514-340-4711 (4870); e-mail: jeanm@polymtl.ca).
Jean Bélanger is with Opal-RT Technologies.
Paper submitted to the International Conference on Power Systems Transients (IPST2011) in Delft, the Netherlands June 14-17, 2011

equation systems. In hybrid analysis, branch voltages and currents can be related as follows

$$\begin{bmatrix} \mathbf{I_{v_x}} \\ \mathbf{V_{i_x}} \\ \mathbf{I_{v_n}} \\ \mathbf{V_{i_n}} \end{bmatrix} = \begin{bmatrix} \mathbf{H_{v_xv_x}} & \mathbf{H_{v_xi_x}} & \mathbf{H_{v_xv_n}} & \mathbf{H_{v_xi_n}} \\ \mathbf{H_{i_xv_x}} & \mathbf{H_{i_xi_x}} & \mathbf{H_{i_xv_n}} & \mathbf{H_{i_xi_n}} \\ \mathbf{H_{v_nv_x}} & \mathbf{H_{v_ni_x}} & \mathbf{H_{v_nv_n}} & \mathbf{H_{v_ni_n}} \\ \mathbf{H_{i_nv_x}} & \mathbf{H_{i_ni_x}} & \mathbf{H_{i_nv_n}} & \mathbf{H_{i_ni_n}} \end{bmatrix} \begin{bmatrix} \mathbf{V_{v_x}} \\ \mathbf{I_{i_x}} \\ \mathbf{V_{v_n}} \\ \mathbf{I_{i_n}} \end{bmatrix} + \begin{bmatrix} \mathbf{H_{v_xa}} & \mathbf{H_{v_xb}} \\ \mathbf{H_{i_xa}} & \mathbf{H_{i_xb}} \\ \mathbf{H_{v_na}} & \mathbf{H_{v_nb}} \\ \mathbf{H_{i_na}} & \mathbf{H_{i_nb}} \end{bmatrix} \begin{bmatrix} \mathbf{V_a} \\ \mathbf{I_b} \end{bmatrix} \tag{1}$$

The above hybrid analysis formulation is specific to this paper and allows to separate nonlinear components from linear components. Bold characters are used hereinafter to denote vectors and matrices. The subscripts are defined as follows: n stands for generic nonlinear or nodal in the particular case, x stands for state variables, v is for voltage ports, i is for current ports, a indicates independent voltage sources and b indicates independent current sources. The vector $\mathbf{I_{v_x}}$, for example, holds the currents of all voltage ports that are extracted from the network as state variables, whereas the vector $\mathbf{I_{v_n}}$ holds the currents of all voltage ports identified as generic nonlinear. The matrix $\mathbf{H}$ is used to relate port variables through network connectivity. The ports are generic components, either capacitors, inductors of nonlinear devices. The term nonlinear is generic and includes linear functions or particular cases, such as short-circuits and open-circuits. It can also contain entire circuits.

Although equation (1) is generic, it is assumed here for simplification, that the solved network has a topological proper-tree. The same assumption is used for the state variable equations.

Equation (1) can be separated into two parts. First the state variable equations

$$\begin{bmatrix} \mathbf{I_{v_x}} \\ \mathbf{V_{i_x}} \end{bmatrix} = \begin{bmatrix} \mathbf{H_{v_xv_x}} & \mathbf{H_{v_xi_x}} \\ \mathbf{H_{i_xv_x}} & \mathbf{H_{i_xi_x}} \end{bmatrix} \begin{bmatrix} \mathbf{V_{v_x}} \\ \mathbf{I_{i_x}} \end{bmatrix} + \begin{bmatrix} \mathbf{H_{v_xv_n}} & \mathbf{H_{v_xi_n}} \\ \mathbf{H_{i_xv_n}} & \mathbf{H_{i_xi_n}} \end{bmatrix} \begin{bmatrix} \mathbf{V_{v_n}} \\ \mathbf{I_{i_n}} \end{bmatrix} + \begin{bmatrix} \mathbf{H_{v_xa}} & \mathbf{H_{v_xb}} \\ \mathbf{H_{i_xa}} & \mathbf{H_{i_xb}} \end{bmatrix} \begin{bmatrix} \mathbf{V_a} \\ \mathbf{I_b} \end{bmatrix} \tag{2}$$

If the inductance and capacitance matrices are included, equation (2) results into the classical state variable equations

$$\begin{bmatrix} \dot{\mathbf{V}}_{\mathbf{v_x}} \\ \dot{\mathbf{I}}_{\mathbf{i_x}} \end{bmatrix} = \begin{bmatrix} \mathbf{A_{v_xv_x}} & \mathbf{A_{v_xi_x}} \\ \mathbf{A_{i_xv_x}} & \mathbf{A_{i_xi_x}} \end{bmatrix} \begin{bmatrix} \mathbf{V_{v_x}} \\ \mathbf{I_{i_x}} \end{bmatrix} + \begin{bmatrix} \mathbf{B_{v_xv_n}} & \mathbf{B_{v_xi_n}} \\ \mathbf{B_{i_xv_n}} & \mathbf{B_{i_xi_n}} \end{bmatrix} \begin{bmatrix} \mathbf{V_{v_n}} \\ \mathbf{I_{i_n}} \end{bmatrix} + \begin{bmatrix} \mathbf{B_{v_xa}} & \mathbf{B_{v_xb}} \\ \mathbf{B_{i_xa}} & \mathbf{B_{i_xb}} \end{bmatrix} \begin{bmatrix} \mathbf{V_a} \\ \mathbf{I_b} \end{bmatrix} \tag{3}$$

The second part holds the nonlinear equations

$$\begin{bmatrix} \mathbf{I_{v_n}} \\ \mathbf{V_{i_n}} \end{bmatrix} = \begin{bmatrix} \mathbf{H_{v_nv_x}} & \mathbf{H_{v_ni_x}} \\ \mathbf{H_{i_nv_x}} & \mathbf{H_{i_ni_x}} \end{bmatrix} \begin{bmatrix} \mathbf{V_{v_x}} \\ \mathbf{I_{i_x}} \end{bmatrix} + \begin{bmatrix} \mathbf{H_{v_nv_n}} & \mathbf{H_{v_ni_n}} \\ \mathbf{H_{i_nv_n}} & \mathbf{H_{i_ni_n}} \end{bmatrix} \begin{bmatrix} \mathbf{V_{v_n}} \\ \mathbf{I_{i_n}} \end{bmatrix} + \begin{bmatrix} \mathbf{H_{v_na}} & \mathbf{H_{v_nb}} \\ \mathbf{H_{i_na}} & \mathbf{H_{i_nb}} \end{bmatrix} \begin{bmatrix} \mathbf{V_a} \\ \mathbf{I_b} \end{bmatrix} \tag{4}$$

At this stage equation (3) is discretized using trapezoidal integration to give

$$\begin{bmatrix} \mathbf{V_{v_x}} \\ \mathbf{I_{i_x}} \end{bmatrix}_{t+\Delta t} = \hat{\mathbf{A}} \begin{bmatrix} \mathbf{V_{v_x}} \\ \mathbf{I_{i_x}} \end{bmatrix}_t + \hat{\mathbf{B}}_\mathbf{s} \begin{bmatrix} \mathbf{V_a} \\ \mathbf{I_b} \end{bmatrix}_t + \hat{\mathbf{B}}_\mathbf{n} \begin{bmatrix} \mathbf{V_{v_n}} \\ \mathbf{I_{i_n}} \end{bmatrix}_t + \hat{\mathbf{B}}_\mathbf{s} \begin{bmatrix} \mathbf{V_a} \\ \mathbf{I_b} \end{bmatrix}_{t+\Delta t} + \hat{\mathbf{B}}_\mathbf{n} \begin{bmatrix} \mathbf{V_{v_n}} \\ \mathbf{I_{i_n}} \end{bmatrix}_{t+\Delta t} \tag{5}$$

where Δt is the integration time-step and the hatted matrices result from the discretization process. Equation (4) for the nonlinear ports is combined with equation (5) to result into

$$\begin{bmatrix} \mathbf{I_{v_n}} \\ \mathbf{V_{i_n}} \end{bmatrix}_{t+\Delta t} = \hat{\mathbf{H}}_1 \begin{bmatrix} \mathbf{V_{v_x}} \\ \mathbf{I_{i_x}} \end{bmatrix}_t + \hat{\mathbf{H}}_2 \begin{bmatrix} \mathbf{V_a} \\ \mathbf{I_b} \end{bmatrix}_t + \hat{\mathbf{H}}_3 \begin{bmatrix} \mathbf{V_{v_n}} \\ \mathbf{I_{i_n}} \end{bmatrix}_t + \begin{bmatrix} \hat{\mathbf{H}}_4 & \mathbf{H_{nab}} \end{bmatrix} \begin{bmatrix} \mathbf{V_a} \\ \mathbf{I_b} \end{bmatrix}_{t+\Delta t} + \begin{bmatrix} \hat{\mathbf{H}}_5 & \mathbf{H_{nn}} \end{bmatrix} \begin{bmatrix} \mathbf{V_{v_n}} \\ \mathbf{I_{i_n}} \end{bmatrix}_{t+\Delta t} \tag{6}$$

At the solution time-point $t+\Delta t$, the history terms and independent source values are known and allow rewriting equation (6) as follows

$$\begin{bmatrix} \mathbf{I_{v_n}} \\ \mathbf{V_{i_n}} \end{bmatrix}_{t+\Delta t} = \begin{bmatrix} \mathbf{I}_{hist} \\ \mathbf{V}_{hist} \end{bmatrix} + \mathbf{Q_n} \begin{bmatrix} \mathbf{V_{v_n}} \\ \mathbf{I_{i_n}} \end{bmatrix}_{t+\Delta t} \tag{7}$$

where *hist* (history) terms are known variables and the matrix $\mathbf{Q_n}$ is the equivalent system matrix.

B. The notion of State-space groups

Equation (7) can be solved through its combination with the nonlinear port functions. Once the vector $\begin{bmatrix} \mathbf{V_{v_n}} & \mathbf{I_{i_n}} \end{bmatrix}^T$ is determined, equation (5) can follow its solution procedure for calculating all state variables at the time-point $t+\Delta t$. Equation (1) can be also applied to a network section instead of the entire network. This approach can be used to create a group of circuit elements combined with the complete network MANA equations using group equation (7).

This method is named hereinafter the state-space-nodal (SSN) method since it combines state-space groups with nodal (MANA) equations.

SSN equations can be also derived starting from the actual state-space equations of a group

$$\begin{aligned} \dot{\mathbf{x}} &= \mathbf{A}_k \mathbf{x} + \mathbf{B}_k \mathbf{u} \\ \mathbf{y} &= \mathbf{C}_k \mathbf{x} + \mathbf{D}_k \mathbf{u} \end{aligned} \tag{8}$$

The column vectors $\mathbf{x}$ and $\mathbf{u}$ are the state variable and input vectors respectively. The column vector $\mathbf{y}$ is the vector of outputs. The state-space matrices $\mathbf{A}_k$, $\mathbf{B}_k$, $\mathbf{C}_k$ and $\mathbf{D}_k$ correspond to the *k*th permutation of switches and piecewise linear device segments. In this way the group equations can

contain ideal switches and nonlinear functions as in a stand-alone state-space solution method.

The discretization of state equations in equation (8) results into

$$\mathbf{x}_{t+\Delta t} = \hat{\mathbf{A}}_k\,\mathbf{x}_t + \hat{\mathbf{B}}_k\,\mathbf{u}_t + \hat{\mathbf{B}}_k\,\mathbf{u}_{t+\Delta t} \tag{9}$$

Equation (9) and the output equations in (8) are refined as follows

$$\mathbf{x}_{t+\Delta t} = \hat{\mathbf{A}}_k\,\mathbf{x}_t + \hat{\mathbf{B}}_k\,\mathbf{u}_t + \begin{bmatrix}\hat{\mathbf{B}}_{k_i} & \hat{\mathbf{B}}_{k_n}\end{bmatrix}\begin{bmatrix}\mathbf{u}_{i_{t+\Delta t}}\\ \mathbf{u}_{n_{t+\Delta t}}\end{bmatrix} \tag{10}$$

$$\begin{bmatrix}\mathbf{y}_{i_{t+\Delta t}}\\ \mathbf{y}_{n_{t+\Delta t}}\end{bmatrix} = \begin{bmatrix}\mathbf{C}_{k_i}\\ \mathbf{C}_{k_n}\end{bmatrix}\mathbf{x}_{t+\Delta t} + \begin{bmatrix}\mathbf{D}_{k_{ii}} & \mathbf{D}_{k_{in}}\\ \mathbf{D}_{k_{ni}} & \mathbf{D}_{k_{nn}}\end{bmatrix}\begin{bmatrix}\mathbf{u}_{i_{t+\Delta t}}\\ \mathbf{u}_{n_{t+\Delta t}}\end{bmatrix} \tag{11}$$

The subscript character *i* refers to internal sources (injections) and the subscript *n* refers to external nodal injections. The combination of the lower row of equation (11) with equation (10) gives

$$\begin{aligned}\mathbf{y}_{n_{t+\Delta t}} &= \mathbf{C}_{k_n}\left(\hat{\mathbf{A}}_k\,\mathbf{x}_t + \hat{\mathbf{B}}_k\,\mathbf{u}_t + \hat{\mathbf{B}}_{k_i}\mathbf{u}_{i_{t+\Delta t}}\right) + \mathbf{D}_{k_{ni}}\mathbf{u}_{i_{t+\Delta t}}\\ &+\left(\mathbf{C}_{k_n}\hat{\mathbf{B}}_{k_n} + \mathbf{D}_{k_{nn}}\right)\mathbf{u}_{n_{t+\Delta t}}\end{aligned} \tag{12}$$

It is apparent that the above equation has an independent term (known variables before solving for $\mathbf{y}_{n_{t+\Delta t}}$) and can be written as

$$\mathbf{y}_{n_{t+\Delta t}} = \mathbf{y}_{k_{hist}} + \mathbf{W}_{k_n}\,\mathbf{u}_{n_{t+\Delta t}} \tag{13}$$

Here the subscript *hist* denotes known variables for the solution of this equation.

When $\mathbf{y}_n$ represents current injections (entering a group) and $\mathbf{u}_n$ is for node voltages, then $\mathbf{y}_{k_{hist}}$ represents history current sources ($\mathbf{i}_{k_{hist}}$) and $\mathbf{W}_{k_n}$ is an admittance matrix. This is called hereinafter a V-type SSN group and it is a Norton equivalent.

When $\mathbf{y}_n$ represents voltages and $\mathbf{u}_n$ holds currents entering a group, then $\mathbf{y}_{k_{hist}}$ represents history voltage sources ($\mathbf{v}_{k_{hist}}$) and $\mathbf{W}_{k_n}$ is an impedance matrix. This is referred to hereinafter as an I-type SSN group and it is a Thevenin equivalent.

In general, it is possible to have both types of groups (V-type and I-type) by rewriting equation (13) as follows

$$\begin{bmatrix}\mathbf{i}_n^{\mathrm{V}}\\ \mathbf{v}_n^{\mathrm{I}}\end{bmatrix}_{t+\Delta t} = \begin{bmatrix}\mathbf{i}_{k_{hist}}\\ \mathbf{v}_{k_{hist}}\end{bmatrix} + \mathbf{W}_{k_n}\begin{bmatrix}\mathbf{v}_n^{\mathrm{V}}\\ \mathbf{i}_n^{\mathrm{I}}\end{bmatrix}_{t+\Delta t} \tag{14}$$

where the superscripts V and I denote V-type and I-type relations respectively. This equation is referred to as a mixed-type group equation. It is equivalent to equation (7) by noticing that V-type relations are voltage ports, I-type relations are current ports and $\mathbf{W}_{k_n} = \mathbf{Q}_{\mathbf{n}}$.

Demonstrating that the new SSN method can be derived from hybrid analysis, provides new confirmation to its theoretical generality. To the author's best knowledge such theoretically demonstrations have not been previously presented in the literature.

C. Interfacing the groups

Once equation (14) is defined for a given group, it can be inserted into the main network equations and simultaneously interfaced with other group equations. This is done using MANA formulation for the main network. In MANA [5],[6],[16]

$$\mathbf{b}_{\mathbf{N}_{t+\Delta t}} = \mathbf{A}_{\mathbf{N}}\,\mathbf{x}_{\mathbf{N}_{t+\Delta t}} \tag{15}$$

where the subscript **N** denotes MANA matrices and vectors, and the vector $\mathbf{x}_{\mathbf{N}}$ can hold both unknown voltages and currents. The upper (V-type) rows of equation (14) can be inserted directly into equation (15) by mapping the group nodes. The lower row (I-type) variables $\mathbf{v}^{\mathrm{I}}_{n_{t+\Delta t}}$ and $\mathbf{i}^{\mathrm{I}}_{n_{t+\Delta t}}$ can be regrouped on the right-hand side and listed in $\mathbf{x}_{\mathbf{N}}$ with coefficients inserted in equation rows of $\mathbf{A}_{\mathbf{N}}$. The history terms of (14) participate in $\mathbf{b}_{\mathbf{N}}$ with a negative sign.

The matrix $\mathbf{A}_{\mathbf{N}}$ can change between solution time-points if the $\mathbf{W}_{k_n}$ matrix of any group changes due to changes in switch positions or in segment positions for piecewise linear devices.

If in the system of equations (8), the equation for $\mathbf{y}$ is modified to include the differential of $\mathbf{u}$ then

$$\mathbf{y} = \mathbf{C}_k\,\mathbf{x} + \mathbf{D}_k\,\mathbf{u} + \mathbf{D}_{1k}\,\dot{\mathbf{u}} \tag{16}$$

and the I-type groups can be avoided. However, the capability to use I-type groups remains useful since in many state-space solvers, such as in [1], the matrix $\mathbf{D}_{1k}$ is not readily available.

Equation (15) does not make any assumptions on the combined group equations. Any number (including zero) of groups can use state-space equations and any number of groups can use MANA (or nodal) equations. A group may contain an arbitrary number of devices. Moreover, MANA equations can contain nonlinear devices solved through an iterative process and independently from state-space equations. The capability to evacuate the solution of nonlinear devices in MANA groups is another important contribution in the proposed method.

D. Steady-state solution

The steady-state solution is found for initializing the time-domain solution. For MANA groups, it is sufficient to use the complex version of (15) [16] for each group. For state-space groups, the state variable equations (8) are solved by replacing the differential operator by Laplace $s = j\,\omega$, with j being the complex operator and ω the steady-state solution frequency in rad/s. Thus the complex version of equation (8) for the solution of state-variables becomes

$$\tilde{\mathbf{X}} = \left(s\mathbf{I} - \mathbf{A}_k\right)^{-1}\left(\mathbf{B}_{k_i}\,\tilde{\mathbf{U}}_i + \mathbf{B}_{k_n}\,\tilde{\mathbf{U}}_n\right) \tag{17}$$

$$\tilde{\mathbf{Y}}_i = \left(\mathbf{C}_{k_i}\,\mathbf{H}\mathbf{B}_{k_i} + \mathbf{D}_{k_{ii}}\right)\tilde{\mathbf{U}}_i + \left(\mathbf{C}_{k_i}\,\mathbf{H}\mathbf{B}_{k_n} + \mathbf{D}_{k_{in}}\right)\tilde{\mathbf{U}}_n \tag{18}$$

$$\tilde{\mathbf{Y}}_n = \left(\mathbf{C}_{k_n}\,\mathbf{H}\mathbf{B}_{k_i} + \mathbf{D}_{k_{ni}}\right)\tilde{\mathbf{U}}_i + \left(\mathbf{C}_{k_n}\,\mathbf{H}\mathbf{B}_{k_n} + \mathbf{D}_{k_{nn}}\right)\tilde{\mathbf{U}}_n \tag{19}$$

where tilde-upper-case vectors are used to denote phasors, **I**

is the identity matrix and $\mathbf{H} = (s\mathbf{I} - \mathbf{A}_k)^{-1}$. Equation (19) is first inserted into the complex version of (15) for finding the nodal solution. It is followed by the solution of equations (17) and (18). The solution of state variables at the time-point $t = 0$ is found by taking the real part of the corresponding phasors. This solution is used to initialize history terms for the following time-point solution with discretized equations (10) and (11).

E. Comparison with state-space and contributions to real-time simulations

The proposed method provides several advantages for solvers based on state-space equations. The clustering approach reduces the size and complexity in the automatic generation of state-space equations for each group. The groups can be solved in parallel and the number of pre-calculated matrix sets for switching topologies can be dramatically reduced. This is particularly important for real-time simulations.

The groups are linked only through the nodal interfacing equations. The computational burden of equation (15) is negligible when compared to much larger group equations.

In the SSN method, the nonlinear functions can be advantageously evacuated into nodal groups [15] thus allowing to program a simultaneous solution much more efficiently than through state-space equations. Due to the reduced number of equations in the iterative process, the SSN method has the potential of introducing iterative solution methodology into real-time solution methods.

It is apparent from the theoretical demonstration and the following validation examples, that the SSN method can be used to separate networks at arbitrary locations.

III. TEST CASES

The method proposed in this paper has been validated using simple and complex systems. In addition to independent programming, the new method has been also implemented in the SimPowerSystems [1] (SPS) tool for Simulink. The reference MANA method is the one in EMTP-RV [16].

A. HVDC system

This system (Fig. 1) is composed of a 1000 MW HVDC link used to transmit power from a 500 kV, 5000 MVA and 60 Hz network to a 345 kV, 10000 MVA and 50 Hz network. The AC networks are modeled by equivalents. The rectifier and the inverter are 12-pulse converters interconnected through a 300 km distributed parameter line (includes propagation delay) and two 0.5 H smoothing reactors. Capacitor banks, harmonic filters (11th and 13th) and high-pass filters for a total of 600 Mvars are used on each converter side. The three-winding transformers are Y-grounded on primary side and Y-Delta on the secondary side. The complete model and data are available in the software SimPowerSystems [1] . The only difference in this design is that the (300 Mvars) capacitor of the filter bank on the rectifier part is split into two parts, one of which is switched.

For the purpose of the test, the following groups are created on the rectifier side:

- Group #1: AC-source and impedance, V-type SSN group
- Group #2: Switched capacitor, I-type SSN group
- Group #3: Fixed filter bank, I-type SSN group
- Group #4: Transformer, thyristor-rectifier and smoothing reactor, V-type SSN group.

The inverter side is simulated using the state-space method of [1].

The test consists of the energization of the DC-link to the nominal current with the 300 Mvars capacitor is switched on at 1.5 s of the simulation interval.

The simulation results are compared to SPS in Fig. 2 to Fig. 4 for a fixed integration time-step of $25\,\mu s$. The match is very close and validates the SSN method. Closer examination of the DC current (see Fig. 3) will show small differences between the two simulation methods. This is normal since any small discrepancy in the thyristor switching methods will cause differences. In the current SPS code it is not possible to access details related to thyristor turn-on/turn-off and reproduce it exactly. The initial implementation based on the SSN method does not use specific switching tricks and the thyristor model is ideal. A low frequency jitter occurs in both methods. This jitter is due to the $25\,\mu s$ sampling time-step for thyristor switching. A solution to this problem has been proposed in [19]. Fig. 5 shows the precision improvement using a time-step of $50\,\mu s$ in SSN.

The same HVDC system can be simulated with 6 additional switched filter banks on the AC bus. This is achieved at a low computational cost since all banks are connected to the same node. The rectifier side Group #4 is now separated into 4 groups (transformer, two bridges and reactor). With the 6 additional capacitor bank groups replacing Group #1, the total number of groups becomes 12. The rank of $\mathbf{A_N}$ in (15) is 11. This stands for three AC bus nodes, 6 transformer secondary side nodes, the node connecting the upper and lower bridges and the left-hand side reactor node. The transmission line model parts are included in the inductor on the left hand-side and in the normal state-space group on the right-hand side.

Different grouping strategies can be used to minimize memory requirements and optimize speed.

The effect of switching banks is apparent on the rectifier firing angle shown in Fig. 6.

B. Breaker test setup

The tested system is shown in Fig. 7. It has been trimmed to simplify the presentation. It is used for testing fault detection and breaker opening under various fault conditions. It is a $50\,\text{Hz}$ and $225\,\text{kV}$ system with short transmission lines modeled as balanced PI sections. The source impedances are decoupled with $R = 1.27\,\Omega$ and $L = 63.5\,\text{mH}$. The PI sections have a capacitance of $1\times10^{-14}\,\text{F/km}$ (diagonal matrix). The positive-sequence resistance and inductance are $60\,\text{m}\Omega/\text{km}$

and $1.27\,\mathrm{mH/km}$ respectively, while the zero-sequence counterpart is three times higher. The system is lightly loaded with all loads having $P = 50\,\mathrm{MW}$ and $Q = 0$. The tested fault locations are identified as F1 to F4. Various fault types with fault resistance can be applied. The tested breakers are BR1 and BR2.

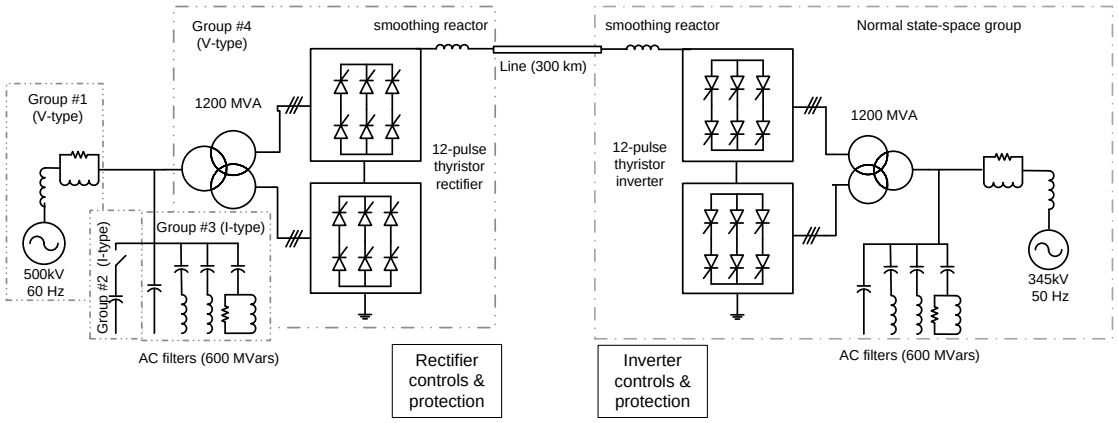

Fig. 1 12-pulse HVDC system

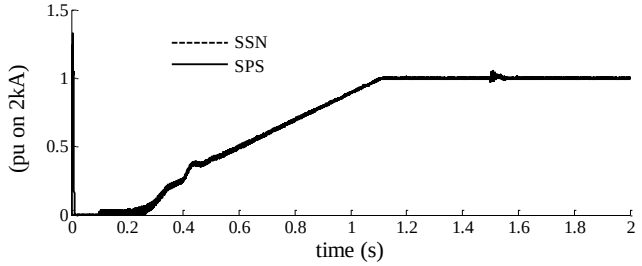

Fig. 2 DC-link current

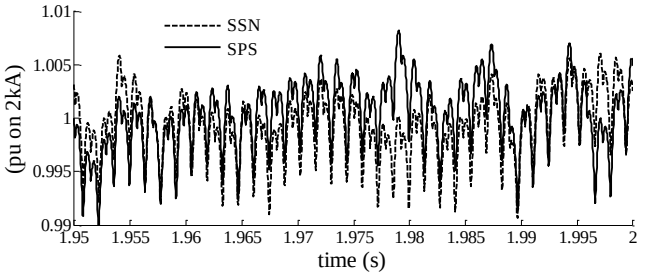

Fig. 3 DC-link current, zoomed interval

The system is decomposed into 5 SSN (SS1 to SS5) groups as identified in Fig. 7. The SS1 group is of mixed-type. There is a total of 9 nodal points. The simulation results for CT1 (BR2) currents with a time-step of $25\,\mu\mathrm{s}$ for a phase-a to phase-b fault occurring at 100 ms at F3, are shown in Fig. 8. The breakers remain closed in this test and the fault disappears at 150 ms. The simulation results with SSN and SPS methods are identical.

The system of Fig. 7 is using PI sections and it is not possible to decouple with propagation delays of transmission line models. This is an important limitation for real-time applications. There are 2 breakers and 4 fault devices. The breakers use 3 switches and the fault devices require 4 switches for modeling various types of faults. This forces the pre-calculation of 2^{22} sets of state-space solution matrices, which is not realizable.

In the SSN approach, the switches are located in independent state-space groups. With the setup of five groups (see Fig. 7), the maximum number of combinations reduces to 2^7 with 4 fault switches and 3 breaker switches in the groups SS1 and SS5.

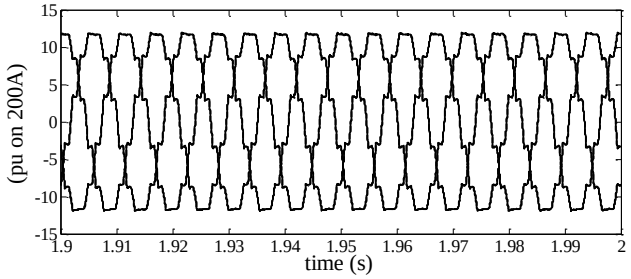

Fig. 4 Rectifier AC currents, SSN (solid line) and SPS (dashed line) methods

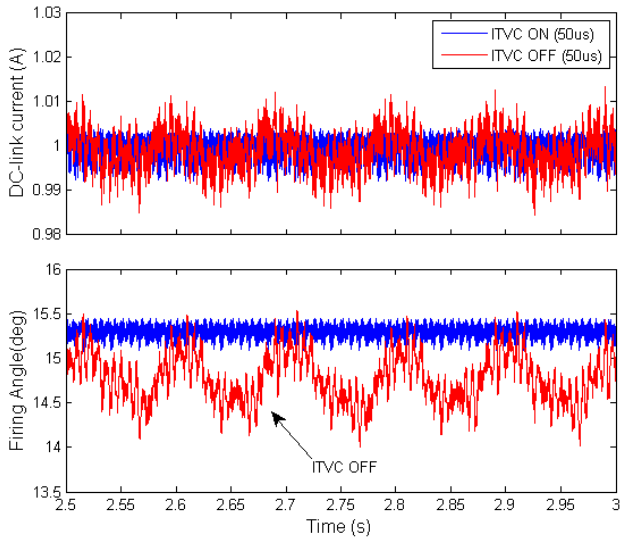

Fig. 5 DC-link current with jitter correction algorithm

C. *Real-time simulation results*

In addition to the off-line simulations presented above, the HVDC system of Fig. 1 and the Breaker test setup of Fig. 7 have been tested in real-time on a target platform [20] comprising a single 3.2 GHz Xeon i7 Quad-core PC running

under RedHat Linux kernel. These tests are using the SPS implementation of the SSN algorithm.

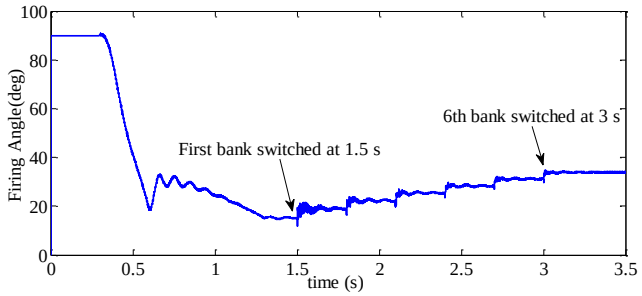

Fig. 6 DC-link rectifier firing angle for AC filter bank energization

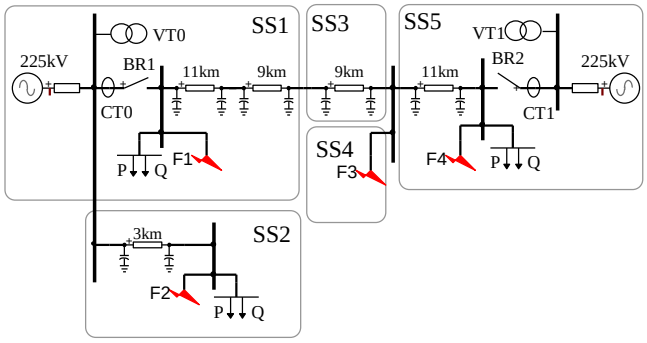

Fig. 7 Breaker test setup, single-line diagram

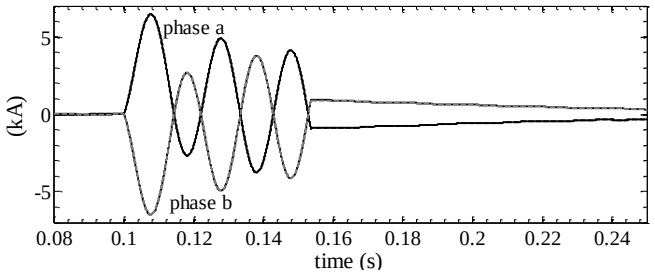

Fig. 8 CT1 current, SSN (solid line) and SPS (dashed line) methods

The HVDC system was simulated with 3 cores: one core for the rectifier side based on the SSN method, the second core for the inverter side based on the state-space approach and the third core was used for simulating the HVDC controls. The worst case time-step reached 10µs with the groups identified in Fig. 1.

The Breaker test setup was simulated on a single core. The worst case condition gives a time-step of 21µs.

The following table summarizes the time-step results. HVDC-6FB identifies the HVDC system with 6 additional filter banks. The worst case condition is suitable for 'hard' real-time simulation, it is the maximum calculation time of all time-steps. The switching events maximize processor un-caching effects. The measurements shown in the table below were performed without I/O devices.

TABLE I Hard real-time time-step

Test case	SSN time-step (µs)	CPUs used (power + control)
HVDC	10	2+1
HVDC-6FB	37	2+1
Breaker test	21	1

IV. CONCLUSION

This paper presented new theoretical demonstrations for a power system simulation method based on the creation of group equations. The group equations can use state-space or MANA equations. All groups are solved simultaneously through a common MANA system.

The grouping of network devices enables to modulate the computational burden between state-space and nodal equations. The paper contributes to the improvement of state-space based off-line and real-time solvers by increasing computational efficiency and eliminating numerical limitations.

REFERENCES

[1] SimPowerSystems, User's Guide, Version 5, The MathWorks Inc., 2009.

[2] D. A. Woodford, A. M. Gole and R. Z. Menzies: "Digital simulation of dc links and ac machines", IEEE Trans. on Power Apparatus and Systems, vol. 102, no. 6, June 1983, pp. 1616-1623.

[3] P. Forsyth, R. Kuffel: "Utility applications of a RTDS® Simulator," 2007 International Power Engineering Conference, IPEC, pp. 112-117.

[4] D. Pare, G. Turmel, J.-C. Soumagne: "Validation of the Hypersim digital real-time simulator with a large AC-DC network," Proc. of IPST (International Power Systems Transients) conference, 2003, New Orleans.

[5] J. Mahseredjian: "Simulation des transitoires électromagnétiques dans les réseaux électriques", Édition 'Les Techniques de l'Ingénieur', Dossier n°D4130, 2008.

[6] J. Mahseredjian and F. Alvarado: "Creating an Electromagnetic Transients Program in MATLAB: MatEMTP". IEEE Transactions on Power Delivery, January 1997, Vol. 12, Issue 1, pages 380-388.

[7] J. R. Martí, L. R. Linares, J. A. Hollman, F. A. Moreira: "OVNI: Integrated software/Hardware Solution for Real-time Simulation of Large Power Systems", Proceedings of the PSCC'02, Sevilla, Spain, June, 2002.

[8] J. A. Hollman, J. R. Martí: "Real Time Network Simulation with PC Clusters,", IEEE Transactions on Power Systems," vol. 18, no. 2, pp. 563-569, May 2003.

[9] J. Mahseredjian, S. Lefebvre and D. Mukhedkar: "Power converter simulation module connected to the EMTP". IEEE Transactions on Power Systems, May 1991, Vol. 6, Issue 2, pages 501-510.

[10] K. Strunz, E. Carlson: "Nested Fast and Simultaneous Solution for Time-Domain Simulation of Integrative Power-Electric and Electronic Systems", IEEE Transactions on Power Delivery", vol. 22, no. 1, pp. 277-287, Jan 2007.

[11] C.Dufour, "Deux contributions à la problématique de la simulation numérique en temps réel des réseaux de transport d'énergie", Ph.D. thesis, Laval University, Québec City, Canada, May 2000.

[12] M. Tiberg, D. Bormann, B. Gustavsen, C. Heitz, O. Hoenecke, G. Muset, J. Mahseredjian, P. Werle: "Generic and Automated Simulation Modeling Based on Measurements", Proc. of IPST (International Power Systems Transients) conference, 2007.

[13] J. Mahseredjian: "State-space equations", July 2005, EMTP-RV documentation.

[14] C. Dufour, S. Abourida, J. Bélanger, V. Lapointe, "InfiniBand-Based Real-Time Simulation of HVDC, STATCOM, and SVC Devices with Commercial-Off-The-Shelf PCs and FPGAs", 32nd Annual Conference

of IEEE Industrial Electronics Society (IECON-06), Paris, France, November 7-10, 2006.

[15] C. Dufour, J. Mahseredjian and J. Bélanger: “A Combined State-Space Nodal Method for the Simulation of Power System Transients”, accepted for IEEE Trans. on Power Delivery, 2011.

[16] J. Mahseredjian, S. Dennetière, L. Dubé, B. Khodabakhchian and L. Gérin-Lajoie, “On a new approach for the simulation of transients in power systems”, Electric Power Systems Research, vol. 77, no. 11, September 2007, pp. 1514-1520.

[17] L. O. Chua and P. M. Lin, “Computer aided analysis of electronic circuits: algorithms and computational techniques”, Prentice Hall, Englewood Cliffs, CA, 1975.

[18] H. C. So: "On the hybrid description of a linear n-port resulting from the extraction of arbitrarily specified elements". IEEE Trans. on Circuit Theory, Vol. 12, pp. 381-387, 1965.

[19] C. Dufour, J. Bélanger, S. Abourida, “Accurate Simulation of a 6-Pulse Inverter With Real Time Event Compensation in ARTEMIS”, Mathematics and Computers in Simulation, vol. 63 , Issue 3-5, pp.161-172, November 2003, ISSN:0378-4754.

[20] RT-LAB, v. 10, Opal-RT Technologies, 2010.